

Isolation of Mesoporous Biogenic Silica from the Perennial Plant *Equisetum hyemale*

Lanny Sapei,[†] Robert Nöske,[‡] Peter Strauch,[‡] and Oskar Paris^{*,†}

Department of Biomaterials, Max-Planck-Institute of Colloids and Interfaces, Research Campus Golm, D-14424 Potsdam, Germany, and Department of Chemistry, University of Potsdam, K-Liebknecht-Str. 24-25, D-14476 Potsdam, Germany

Received October 17, 2007. Revised Manuscript Received January 2, 2008

The structure-conserving isolation of biogenic silica from the perennial plant *Equisetum hyemale* is investigated using several chemical and thermal treatments. X-ray diffraction and small-angle X-ray scattering are employed to characterize crystalline phases and nanostructure of the resulting material, respectively, complemented by nitrogen sorption for porosity analysis. A mild, long-time treatment of the native dry plant with hydrogen peroxide leads to a fully intact silica replica of the outer epidermis of the plant, exhibiting a pronounced nanostructure with a high internal surface area. A similar material with even higher surface area is obtained by a short-time chemical treatment with hydrochloric acid followed by a calcination treatment. The highest grade silica with largest surface area ($> 400 \text{ m}^2/\text{g}$) is obtained by calcination at 500°C . Omitting the HCl treatment yields a much denser material with rather low surface area, and the total porosity decreases with increasing temperature and vanishes at 750°C . Additionally, a transformation from amorphous silica to cristobalite is observed at this temperature. This unfavorable behavior is mainly attributed to the interaction of the biogenic silica with alkali ions present in the native plant, which disrupts the silica network and leads to the collapse of the pore structure.

Introduction

The rich structural hierarchy of plants permits to obtain hierarchical porous structures which can be expected to show a better performance in fields such as heterogeneous catalysis or separation due to macroscopic directionality of the pores, high selectivity, and faster kinetics. Hence, “biomorphous” materials have been synthesized by using plants as templates to obtain micrometer¹ and nanometer^{2,3} replication of the hierarchical plant structure. In some higher plants such as grasses (*Gramineae*) and horsetail (*Equisetum*), inorganic material is already present abundantly in the form of amorphous silica.⁴ Gentle isolation of this biogenic silica may lead to novel nanostructured materials that also resemble parts of the original hierarchical plant structure. Moreover, given the fact that cheap and environmental-friendly production of mesoporous silica with high surface area is highly desirable in many fields of materials industries, silica from plant resources may be simply an attractive alternative to synthetically produced silica. Rice husks for instance contain very high amounts of biogenic silica which can be extracted from the biological template and purified.⁵ Because of the

abundant availability of rice husk silica, several applications as filler in rubbers and plastics or in cement production have been reported so far.^{6,7} It has also been shown⁸ that high-grade amorphous mesoporous silica with large surface area can be obtained from rice husks, if they are subjected to a treatment in hydrochloric acid before calcination.

Among the higher plants, *Equisetum spp.* commonly also known as horsetail or scouring rush, is one of the strongest silica accumulators with silica content up to 25% of the total plant dry weight.⁹ The silica deposition is almost exclusively restricted to the outer epidermal layer of the plant stem and leaves, and it has been shown that silica is intimately connected to the plant biopolymers.^{10,11} Biogenic silica in *Equisetum* is almost exclusively amorphous with a pronounced nanostructure,^{11,12} making it an interesting candidate as a source of inorganic silicon-containing materials such as silica or SiC. There were some recent attempts to use *Equisetum* as a biological template for zeolite macrostructures^{13–15} and for direct carbothermal synthesis of β -SiC.^{16,17}

* Corresponding author. E-mail: Oskar.Paris@mpikg.mpg.de.

[†] Max-Planck-Institute of Colloids and Interfaces.

[‡] University of Potsdam.

- (1) Zampieri, A.; Schwieger, W.; Zollfrank, C.; Greil, P. In *Handbook of Biomineralization*; Behrens, P., Bäuerlein, E., Eds.; Wiley-VCH: Weinheim, 2007; Vol. 2, pp 255–288.
- (2) Shin, Y. S.; Liu, J.; Chang, J. H.; Nie, Z. M.; Exarhos, G. *Adv. Mater.* **2001**, *13* (10), 728–732.
- (3) Deshpande, A.; Burgert, I.; Paris, O. *Small* **2006**, *2*, 994–998.
- (4) Mann, S.; Perry, C. C.; Williams, R. J. P.; Fyfe, C. A.; Gobbi, G. C.; Kennedy, G. J. *J. Chem. Soc., Chem. Commun.* **1983**, (4), 168–170.
- (5) Nunn, G. R. Soluble biogenic silica and applications using same. International Patent WO 2005-AU188 20050214, 2005.

(6) Sun, L. Y.; Gong, K. C. *Ind. Eng. Chem. Res.* **2001**, *40* (25), 5861–5877.

(7) Chandrasekhar, S.; Satyanarayana, K. G.; Pramada, P. N.; Raghavan, P.; Gupta, T. N. *J. Mater. Sci.* **2003**, *38* (15), 3159–3168.

(8) Real, C.; Alcala, M. D.; Criado, J. M. *J. Am. Ceram. Soc.* **1996**, *79* (8), 2012–2016.

(9) Perry, C. C.; Fraser, M. A. *Philos. Trans. R. Soc. London, Ser. B* **1991**, *334* (1269), 149–157.

(10) Perry, C. C.; Keeling-Tucker, T. *J. Biol. Inorg. Chem.* **2000**, *5* (5), 537–550.

(11) Sapei, L.; Gierlinger, N.; Hartmann, J.; Nöske, R.; Strauch, P.; Paris, O. *Anal. Bioanal. Chem.* **2007**, *389*, 1249–1257.

(12) Holzhüter, G.; Narayanan, K.; Gerber, T. *Anal. Bioanal. Chem.* **2003**, *376* (4), 512–517.

(13) Valtchev, V.; Smaih, M.; Faust, A. C.; Vidal, L. *Angew. Chem., Int. Ed.* **2003**, *42* (24), 2782–2785.

However, unlike rice husks, there are practically no detailed investigations considering *Equisetum* as a source of biogenic silica.

In the present paper we provide a comprehensive investigation of the silica structure obtained from *Equisetum hyemale* after different chemical and thermal treatments. X-ray diffraction (XRD) is used to identify different inorganic phases, and small-angle X-ray scattering (SAXS) delivers quantitative nanostructural parameters including the total surface area. SAXS is complemented by N₂ sorption, which allows obtaining complementary information about open and closed porosity. We demonstrate that the macroscopic plant structure can be retained to a large extent and that a chemical treatment prior to calcination drastically enhances the surface area of the obtained silica.

Experimental Section

Materials. *Equisetum hyemale* shoots were derived from the Botanical Garden (Drachenberg) at the University of Potsdam, Germany. The plant stalks were dried at 105 °C, and part of them was milled to a powder before further processing. Two series of specimens were prepared from both the intact and the milled plant stalks. Series i: calcination in air at seven different temperatures (300, 350, 400, 450, 500, 600, and 750 °C) at a heating rate of 1 K/min for 48 h. This led to materials denoted as “ash” in the following. Series ii: treatment in 10% HCl at boiling temperature for 2 h, followed by a calcination treatment at the same temperatures as in series i. These samples are referred to as “biogenic silica”. One additional sample was prepared by a mild treatment of a native *E. hyemale* stalk with 30% H₂O₂ for 18 months at room temperature.

The average ash content determined gravimetrically after calcination of the native *E. hyemale* internodes was about 20% of the total dry weight, from which about 60 wt % could be attributed to pure silica after the HCl treatment. An elemental analysis of the ash by X-ray fluorescence analysis (XRF) showed in addition to Si in particular K and Ca with a concentration in the order of 1 wt % each and somewhat smaller but non-negligible amounts of Na, Mg, P, S, and Cl. After HCl treatment and subsequent calcination, all these elements were present only in trace amounts, indicating that this chemical treatment was sufficient to efficiently remove all the inorganic impurities. The skeletal density of the silica was determined for the samples calcined at 600 °C with a pycnometer. The measured values of $\rho = 2.4 \text{ g/cm}^3$ and $\rho = 2.1 \text{ g/cm}^3$ for the ash and the HCl-treated samples, respectively, were assumed to be constant over the temperature range 300–750 °C. For the HCl-treated, noncalcined sample the density was estimated to be $\rho = 1.7 \text{ g/cm}^3$ from the known fractions of remaining organic matrix ($\rho \approx 1.5 \text{ g/cm}^3$) and silica ($\rho \approx 2.1 \text{ g/cm}^3$).

Experimental Methods. The nonpowdered specimens were examined with a field emission environmental scanning electron microscope (SEM) (FESEM, Quanta 600F, FEI Co.) in low-vacuum mode at 3 keV. The powdered samples were investigated with X-ray diffraction (XRD), small-angle X-ray scattering (SAXS), and nitrogen sorption. For the SAXS measurements, the powders were

pressed to pellets with 0.2 mm thickness to enable scattering in transmission geometry with a well-defined powder volume in the X-ray beam.

XRD experiments were conducted on a powder diffractometer (D8, Bruker AXS) with a sealed tube X-ray generator in θ – θ geometry. A parabolically bent, graded multilayer (Göbel mirror) was used for beam parallelization and for monochromatization (Cu K α radiation, wavelength $\lambda = 0.154 \text{ nm}$). Data were collected with a solid-state detector (Sol-X, Bruker AXS) in steps of $\Delta(2\theta) = 0.05^\circ$. The scattering angle 2θ was converted into the modulus of the scattering vector q ($q = 4\pi \sin(\theta)/\lambda$).

SAXS measurements were carried out on a NanoStar instrument (Bruker AXS) with a sealed tube X-ray generator operated at 40 kV and 35 mA. A parallel, monochromatic X-ray beam with wavelength $\lambda = 0.154 \text{ nm}$ was provided by two cross-coupled Göbel mirrors. Data were collected with a single photon counting area detector (HiStar, Bruker AXS). Two sample–detector distances of 260 and 1050 mm were used, covering overlapping ranges of scattering vectors q from $0.1 \text{ nm}^{-1} < q < 10 \text{ nm}^{-1}$. Since there was no azimuthal anisotropy of the 2D SAXS patterns, they were azimuthally averaged to obtain one-dimensional scattering profiles of the intensity versus the length of the scattering vector q , and the instrument-related background was subtracted from each data set. The SAXS data were further normalized with respect to measurement time, sample transmission, and sample thickness.

Nitrogen sorption measurements were carried out at 77 K on an Autosorb-1 instrument (Quantachrome Instruments).

Data Treatment. The specific pore volume (V_p) and specific surface area per unit sample mass (σ_{BET}) are derived from the nitrogen sorption isotherms by standard evaluation techniques.¹⁸ An average pore size is evaluated from these two parameters by $D_p = 4V_p/\sigma_{\text{BET}}$, and the pore volume fraction (porosity Φ) is given by $\Phi = V_p/(V_p + 1/\rho)$, with ρ being the skeletal density of the silica material.

One advantage of using SAXS over N₂ sorption is that also closed pores not accessible through nitrogen sorption can be measured. Under the assumption of a two-phase system with sharp interfaces, a correlation length $T = 4I/\pi P = 4\Phi(1 - \Phi)/S$ can be derived from SAXS.¹⁹ Here, $\tilde{I} = \int_0^\infty q^2 I(q) dq = K\pi\Phi(1 - \Phi)$ is the integrated SAXS intensity, and $P = \lim_{q \rightarrow \infty} (q^4 I(q)) = KS$ is the Porod constant derived from the limiting q^{-4} behavior of the SAXS intensity at large q values. S is the total pore surface per unit volume, and K is a constant depending on the instrumental setup and on the mean electron density of the matrix. The mean chord length of the pores (pore size) from SAXS is given by $I_p = T/(1 - \Phi)$,^{19,20} and a comparison with the pore size from N₂ sorption implies that $I_p = D_p$. The total surface area and the volume fractions of pores and matrix can be independently deduced from the SAXS data only if the constant K is known. If the volume fraction Φ is known independently, the total specific surface area can be derived from SAXS without the knowledge of K by $\sigma_{\text{SAXS}} = 4\Phi/\rho T$.²⁰

Results

Figure 1 shows representative SEM images of the outer surface of internodes of *E. hyemale* for the native plant (a) and after the various chemical or/and thermal treatments (b–d). A treatment with 30% H₂O₂ for 18 months considered

(14) Valtchev, V. P.; Smaih, M.; Faust, A. C.; Vidal, L. *Chem. Mater.* **2004**, *16* (7), 1350–1355.

(15) Valtchev, V.; Smaih, M.; Faust, A. C.; Vidal, L. *Stud. Surf. Sci. Catal.* **2004**, *154*, 588–592.

(16) Nöske, R.; Horn, I. Verfahren zur Herstellung von Siliziumkarbid aus nachwachsenden Rohstoffen. German Patent DD 100 20 626, 2001.

(17) Strauch, P.; Lehmann, S.; Nöske, R. In *Progress in Coordination and Bioinorganic Chemistry*; Melnik, M., Sirota, A., Eds.; Slovak Technical University Press: Bratislava, 2003; pp 329–342.

(18) Sing, K. S. W.; Everett, D. H.; Haul, R. A. W.; Moscou, L.; Pierotti, R. A.; Rouquerol, J.; Siemieniowska, T. *Pure Appl. Chem.* **1985**, *57* (4), 603–619.

(19) Glatter, O.; Kratky, O. *Small-Angle X-ray Scattering*; Academic Press: New York, 1983.

(20) Smarsly, B.; Antonietti, M.; Wolff, T. *J. Chem. Phys.* **2002**, *116* (6), 2618–2627.

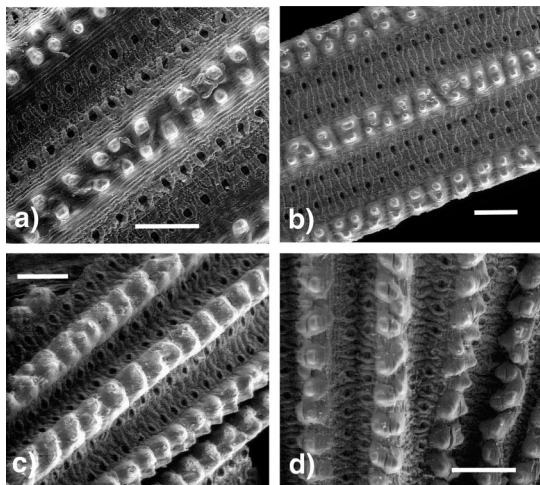


Figure 1. SEM images from *E. hyemale* internodes: (a) native plant; (b) H_2O_2 -treated sample; (c) native *E. hyemale* calcined at 400 °C; (d) HCl-treated *E. hyemale* calcined at 400 °C. The bar is 300 μm in all images.

the use of hydrogen peroxide as a powerful oxidizer for both organic and inorganic substances without affecting silica, with the additional benefit that the only byproduct is water. A very thin and fully transparent continuous layer remained after the treatment. The ribs occupied by two conspicuous parallel rows of knobs as well as the rows of stomata lying on each flank of the ribs reflect perfectly the original morphology of the epidermal layer (compare parts a and b of Figure 1). Such an absolutely perfect replication is not given for the heat-treated samples (Figure 1c,d), where the two rows of knobs have almost merged due to shrinkage. Nonetheless, monolithic silica replicas which still largely represent the original stalk surface structure of the native *E. hyemale* are obviously obtained also after heat treatment at 400 °C (Figure 1c,d).

X-ray diffraction patterns from the powdered specimens are shown in Figure 2. A broad peak at around $q = 15.5 \text{ nm}^{-1}$ indicates the presence of amorphous silica as a major component. This diffuse scattering is overlapped by broad reflections from nanocrystalline cellulose in both the native (Figure 2a) and the HCl-treated *E. hyemale* samples (Figure 2b) before thermal treatment (see the 110/ $\bar{1}$ 10 doublet at $q \approx 11 \text{ nm}^{-1}$, the 200 reflection at $q = 16.2 \text{ nm}^{-1}$, and the 004 reflection at $q = 24.3 \text{ nm}^{-1}$). Additionally, reflections from α -quartz were observed in the HCl-treated sample (Figure 2b), and indications for the presence of some α -quartz are also seen in the native specimen (Figure 2a) before heat treatment. Quartz is the only crystalline component detected in the HCl-treated biogenic silica samples and is present for all temperatures together with the broad maximum from amorphous silica. The amount of α -quartz can be roughly estimated by evaluating the ratio of the integrated intensity from Bragg peaks and from the total integrated scattering intensity, yielding less than 7% α -quartz. In contrast to the HCl-treated sample, the ash specimens display a series of additional sharp Bragg reflections (Figure 2a). Crystalline phases that could unambiguously be determined via a qualitative phase analysis are α -quartz (SiO_2), calcite (CaCO_3), and potassium chloride (KCl). The few reflections that could not be indexed are attributed to some

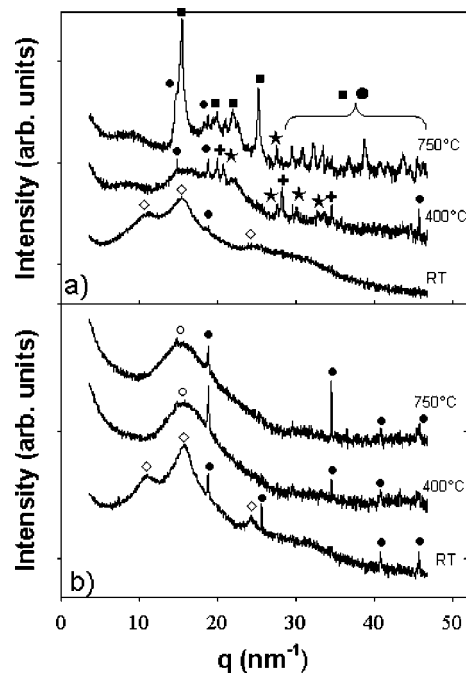


Figure 2. XRD patterns from native (a) and HCl-treated *E. hyemale* (b) at room temperature (RT) as well as for the ash and the biogenic silica for two selected calcination temperatures of 400 and 750 °C (indicated). Different crystallographic phases that could uniquely be assigned are indicated by the different symbols: ◇, cellulose; ○, amorphous silica; ●, α -quartz; ■, cristobalite; +, KCl; ★, CaCO_3 .

minor, more complex phases. The diffraction patterns of the ash appear very similar in the temperature interval between 300 and 500 °C. At 600 °C, new reflections from the silica polymorph cristobalite start to be visible (data not shown). At 750 °C finally, most of the amorphous silica has been transformed into cristobalite as seen by the corresponding reflections and the missing broad hump from amorphous silica in Figure 2a. It is also interesting to note that the reflections from the inorganic compounds (except quartz) are barely visible in the native sample before heat treatment, which indicates that these phases might have been formed only after the thermal treatment. The XRD pattern from the H_2O_2 specimen (not shown) exhibited only the peak of amorphous silica together with some minor sharp reflections that could be attributed to calcium oxalate and α -quartz. No cellulose reflections could be detected in this sample, indicating that all organic substances were successfully removed. This was additionally checked with FTIR spectroscopy.

The SAXS profiles from the native and the HCl-treated specimens are shown in Figure 3a. A constant background was subtracted from each data set. The scattering profile of the dry native *E. hyemale* specimen displays a shoulder at around 2 nm^{-1} , with a clear minimum at about $4\text{--}5 \text{ nm}^{-1}$. This is the fingerprint of the small-angle scattering from crystalline cellulose fibrils of about 2 nm diameter within an amorphous biopolymer matrix²¹ typically found in higher plants. There is a strong increase of the intensity toward small q , reaching limiting q^{-4} behavior at very small q . This indicates the presence of very large ($>50 \text{ nm}$) heterogene-

(21) Jakob, H. F.; Fengel, D.; Tschegg, S. E.; Fratzl, P. *Macromolecules* **1995**, 28 (26), 8782–8787.

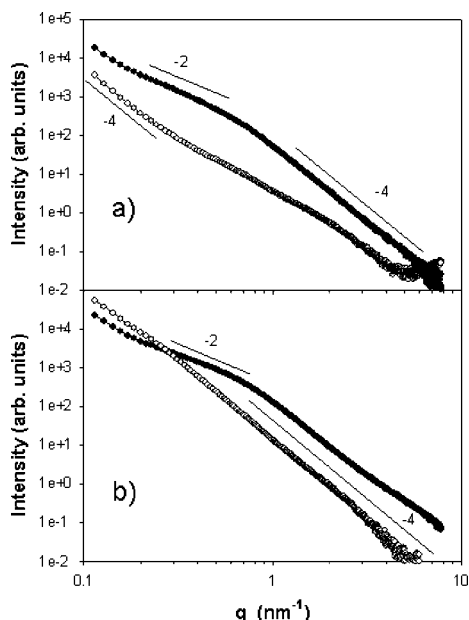


Figure 3. SAXS profiles from native (open circles) and the HCl-treated (black circles) *E. hyemale* measured before calcination (a) and after calcination at 400 °C (b). The lines indicate power law behavior of the profiles with q^{-4} and q^{-2} regions.

ities, which may be identified as large pores and microcracks due to the drying process. The scattering signal in between (0.2–2 nm⁻¹) is hard to interpret due to the fact that there are contributions from the different cell wall polymers and also from silica. After HCl treatment, the scattering profile looks considerably different despite the fact that the cellulose fibrils are not affected by the treatment (see the XRD profile in Figure 2b). It is well-known that the scattering contrast changes upon chemical treatment of plant cell walls,²² and we can assume that the HCl treatment attacks and removes efficiently hemicelluloses and pectin in *E. hyemale*. Recent work^{11,23} has shown that silica in *E. hyemale* is intimately connected to polysaccharides, presumably hemicelluloses and pectin. The change in the SAXS profile upon HCl treatment of *E. hyemale* can therefore be understood by a strong increase of the scattering contribution of silica as compared to the native plant, by a change of the respective contrast contribution. Replacing a hypothetical scattering contrast $\Delta b^2 = (b_{\text{SiO}_2} - b_{\text{M}})^2$ between silica and organic matrix in the native plant by $\Delta b^2 = (b_{\text{SiO}_2})^2$ between silica and pores in the HCl-treated specimen would indeed lead to an increase of the contrast by more than an order of magnitude. (The electron densities were estimated to be $b_{\text{M}} \approx 5.0 \times 10^{23} \text{ e}^-/\text{cm}^3$ and $b_{\text{SiO}_2} \approx 6.6 \times 10^{23} \text{ e}^-/\text{cm}^3$.²²) Therefore, we suggest that the SAXS signal from the HCl-treated specimen is primarily due to the scattering from a highly porous silica framework. This interpretation is supported by the SAXS patterns from the calcined biogenic silica samples, which are almost identical to the uncalcined HCl-treated specimen for all temperatures (see Figure 3b). The q^{-4} behavior at large q with a crossover at around 0.5–1 nm⁻¹ indicates scattering from sharp interfaces with a typical correlation length below 10 nm. Furthermore, there is a q^{-2} region at

Table 1. Structural Parameters Derived from Nitrogen Sorption and SAXS for the Noncalcined Samples

	native	HCl-treated	H ₂ O ₂ -treated
σ_{BET} (m ² /g)	0	56	242
V_{p} (cm ³ /g)	0	0.12	0.99
Φ	0	0.17	0.68
D_{p} (nm)		8.3	16.5
T (nm)	1.56	3.04	4.45
l_{p} (nm)		3.65	13.8
σ_{SAXS} (m ² /g)		128	290

low q , which suggests platelike structures (e.g., slitlike pores)¹⁹ in the HCl-treated specimens. In contrast to the biogenic silica samples, the ash samples treated above 350 °C exhibit SAXS profiles with pure Porod scattering, i.e., a decay with q^{-4} over almost 2 orders of magnitude in q (Figure 3b). This means that there is no specific length scale of porosity in these specimens lower than about 50 nm. Additionally, in the ash samples the total intensity decreases with increasing temperature, indicating a decrease of the total surface area upon calcination.

These structural results from SAXS are corroborated by the nitrogen sorption measurements. While the native *E. hyemale* specimen did not show any measurable N₂ uptake, the HCl-treated sample prior to any thermal treatment exhibited already a pore volume of 0.12 cm³/g and a total surface area of 56 m²/g (Table 1). The H₂O₂ sample (data not shown) exhibited a SAXS pattern somewhat similar to the HCl-treated specimen and exhibited a considerably larger pore volume (0.99 cm³/g) and BET surface area (242 m²/g) (Table 1). Figure 4 compares the sorption isotherms and the corresponding pore size distributions for the ash and the biogenic silica samples after calcination at 400 °C. All calcined HCl-treated samples displayed a H3-type hysteresis loop consistent with slitlike mesopores.¹⁸ The corresponding pore size distribution from a BJH analysis of the sorption isotherms shows a narrow size distribution peaked at around 6 nm. For comparison, the calcined, untreated *E. hyemale* specimen shows a much lower N₂ uptake with almost no hysteresis, indicating the absence of well-defined mesopores. The size distribution is broad and shows no particular peak that would be indicative of a narrow distribution of mesopores.

Quantitative structural parameters derived from SAXS and nitrogen sorption are summarized in Table 1 for the native and the chemically treated samples and in Figure 5 for the ash and the biogenic silica samples as a function of

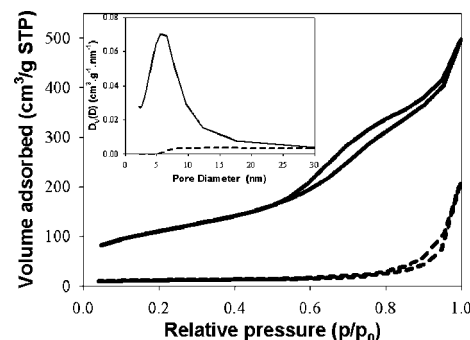


Figure 4. N₂ sorption isotherms for the ash (dashed line) and the biogenic silica (solid line), both calcined at 400 °C. The inset shows the corresponding pore size distributions obtained from a BJH analysis.

(22) Jungnikl, K.; Paris, O.; Fratzl, P.; Burgert, I. *Cellulose*, in press.

(23) Gierlinger, N.; Sapei, L.; Paris, O. *Planta*, in press.

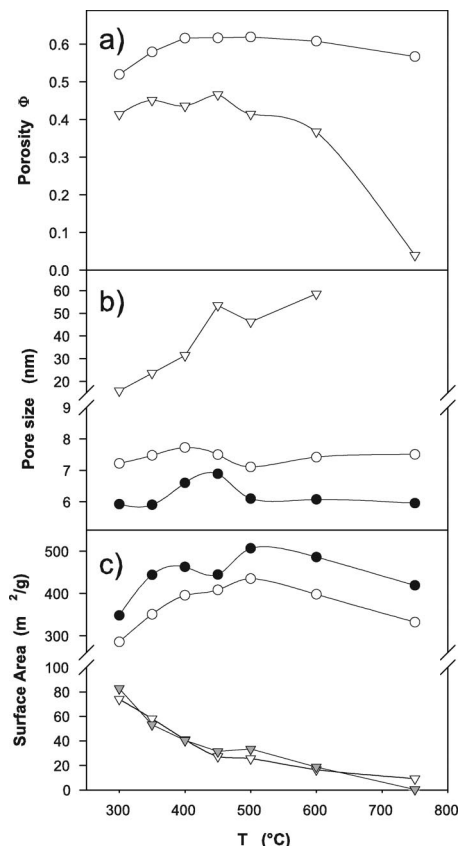


Figure 5. (a) Porosity Φ , (b) pore size D_p (from N_2 sorption) and l_p (from SAXS), and (c) total surface area as a function of calcination temperature. Triangles denote the ash and circles denote the biogenic silica specimens. Open symbols correspond to values derived from N_2 sorption data and solid symbols to values from SAXS. The gray symbols in (c) correspond to the Porod constant derived from SAXS multiplied by a common constant.

calcination temperature. There is obviously a large difference in these parameters between the calcined HCl-treated and the ash samples. First, the BET surface of the biogenic silica samples is significantly higher as compared to the ash samples for all temperatures, exhibiting a maximum of about $400 \text{ m}^2/\text{g}$ at $T = 500 \text{ }^{\circ}\text{C}$ (Figure 5c). Second, for the ash samples both the BET surface and the pore volume fraction decrease strongly with increasing temperature (Figure 5a,c), suggesting the collapse of existing mesopores. Third, the mean pore size D_p derived from nitrogen sorption stays almost constant at about 7.5 nm up to $750 \text{ }^{\circ}\text{C}$ for the biogenic silica samples, while D_p increases strongly with temperature for the ash samples. These general findings are largely supported by the parameters derived from SAXS for the HCl-treated samples (black symbols in Figure 5b,c). The values were derived using the parameter T from SAXS and the porosity Φ from N_2 sorption. The SAXS pore size l_p is slightly smaller, and the total surface area σ_{SAXS} is slightly larger (up to about 20%) as compared to the corresponding values from nitrogen sorption. This might indicate a small amount of closed pores or some very small micropores that are not accessible to nitrogen sorption. Nevertheless, the temperature dependence is very similar for the SAXS and the N_2 sorption data, and even the small dip at $450 \text{ }^{\circ}\text{C}$ is reproduced by both methods.

For the ash samples no value of the T parameter could be obtained due to the fact that the q^{-4} power-law behavior of

the entire scattering profiles (see Figure 3b) prevents a reliable extrapolation of the integrated intensity toward $q = 0$. Therefore, the corresponding values for l_p are omitted in Figure 5b. However, we can compare the relative trend of the Porod constant derived from SAXS with the BET surface area, which is shown in Figure 5c by the gray symbols. Remarkably, the Porod constant from SAXS resembles exactly the same temperature trend as the BET surface area also for the ash samples.

Discussion and Conclusion

We have shown recently that *Equisetum hyemale* internodes contain about 14 wt % silica, which is located almost exclusively at the outer epidermis as a thin continuous layer.^{11,23} Apart from the knob tips which contain pure hydrated amorphous silica over a small region, the concentrations are somewhat lower in the rest of the layer. Here, the silica is strongly associated with the plant biopolymers which most probably act as templating agents during silica deposition. The silica is mostly amorphous as revealed by Raman spectroscopy and XRD, and some small amounts of quartz might arise from dust contaminations. These results^{11,23} are largely corroborated by the present work. The N_2 inaccessibility and a very low Porod constant indicate a negligible porosity in the native plant, supporting the intimate connection of the plant biopolymers with the silica at the scale of a few nanometers. Moreover, removing the biopolymers in *E. hyemale* by a very mild, long-term treatment with H_2O_2 reveals an intact perfect silica replica of the original plant surface (Figure 1b). The obtained material is mesoporous with a surface area of $\sigma_{\text{BET}} \approx 250 \text{ m}^2/\text{g}$. These mesopores are most probably the result of the selective removal of biopolymers and inorganic impurities from the silica/biopolymer nanocomposite.

Such long-term treatments are however not very useful for an effective and economic isolation of silica from *E. hyemale*, and thus, thermal treatment in an oxidizing atmosphere was also considered to remove the organic matrix. However, calcination in air at a temperature of $300 \text{ }^{\circ}\text{C}$ (i.e., the lowest possible temperature to remove cellulose²⁴) gives a total pore surface area of only about $80 \text{ m}^2/\text{g}$. Moreover, the surface area decreases continuously with increasing calcination temperature to a value close to zero at $750 \text{ }^{\circ}\text{C}$, and the amorphous silica is transformed into crystalline cristobalite at this temperature. HCl treatment of the native plants prior to calcination not only removes effectively inorganic impurities such as K and Ca but also dissolves pectin,²⁵ hemicelluloses,²⁶ and amorphous cellulose²⁷ within the organic matrix. Additionally, hydrolysis of anhydrous silica accumulated in the continuous layer adjacent to the epidermal cell wall¹¹ may take place during this acid leaching. As a consequence of this treatment, a

(24) Zickler, G. A.; Wagermaier, W.; Funari, S. S.; Burghammer, M.; Paris, O. *J. Anal. Appl. Pyrol.* **2007**, *80* (1), 134–140.

(25) Trofimova, N. S.; Zabivalova, N. M.; Bochek, A. M.; Novoselov, N. P. *Russ. J. Appl. Chem.* **2001**, *74*, 1924–1927.

(26) Smirnova, L. G.; Grunin, Y. B.; Krasil'nikova, S. V.; Zaverkina, M. A.; Bakieva, D. R.; Smirnov, E. V. *Colloid J.* **2003**, *65* (6), 778–781.

(27) Zhang, Y. H. P.; Himmel, M. E.; Mielenz, J. R. *Biotechnol. Adv.* **2006**, *24* (5), 452–481.

mesoporous material is obtained without any temperature treatment in a relatively short time, even though the BET surface area is considerably lower as compared to the H_2O_2 -treated specimen. It is worth mentioning that the surface area obtained from SAXS for this material is by more than a factor of 2 larger than the BET surface area (Table 1). This indicates a considerable amount of closed pores after HCl treatment, which may be explained by a rearrangement of the remaining crystalline cellulose as a result of drying after the chemical treatment, closing some of the pores again. After calcination of the HCl-treated samples the total surface area σ_{SAXS} increased considerably, reaching a maximum value of $500 \text{ m}^2/\text{g}$ at 500°C , while the pore size l_p increased roughly by a factor of 2. The porosity is now mostly open; i.e., the surface areas determined from SAXS and BET almost coincide. We interpret this as the effective removal of all remaining biopolymers without changing or destroying the structural integrity of the biogenic silica network. The structure of the biogenic silica is similar for the whole temperature range between 300 and 750°C , with just slightly lower values of the pore surface on either side. Figure 1 demonstrates impressively that not only the nanostructure but also the whole hierarchical structure of the original plant up to the macroscopic level can be retained.

What needs to be eventually explained is the instability of the porous silica structure upon calcination without prior HCl treatment. The most probable reason is the interaction of silica with the inorganic impurities. This hypothesis is underlined by the fact that the ash of *E. hyemale* was transformed into cristobalite already at 750°C , while no such transformation was found for the HCl-treated specimens. It is well-known that sodium and potassium can lower the crystallization temperature of amorphous silica considerably, leading to the formation of cristobalite at temperatures as low as 800°C .²⁸ Real et al.⁸ compared the surface area of silica derived from rice husks with and without prior HCl treatment and obtained similar results as in the present work, though their total surface area was lower. They attributed the collapse of the pore structure in rice husks upon calcination to the interaction with K^+ ions. Later on, the same group provided some evidence from XAFS measurements²⁹ that potassium oxide leads to the disruption of the SiO_4 network and the formation of chainlike structures of non-bridging oxygen, which may qualitatively explain the instability of the silica network upon thermal treatment. Alternatively, Krishnarao et al.³⁰ explained the low surface

area of calcined untreated rice husk by the surface melting of silica particles in the presence of potassium impurities. To prove their hypothesis, they impregnated also the acid-leached rice husks with $4 \text{ wt } \% \text{ K}_2\text{CO}_3$ followed by calcination and found similarly low surface area as for the untreated samples. Even though the concentration of potassium is much lower in *E. hyemale* as compared to rice husk, it is the most abundant inorganic element present together with calcium. It seems therefore plausible that similar influences of alkali ions are responsible for the pore collapse in *E. hyemale*, although the detailed mechanisms are still unclear. Besides the unfavorable action of the alkali ions, another influencing factor for the stability of the silica structure may be the initial pore opening by the HCl treatment. Since about 60% of the total mass was removed by the treatment, a large accessible surface is present already prior to the thermal treatment. This allows volatile reaction products to leave the solid framework without the creation of large internal pressure and associated stresses upon thermal treatment, which in the case of the ash might be partly responsible for the collapse of the pore structure.

In conclusion, the results of the present investigation demonstrate that high grade silica with slitlike pores of about $6\text{--}7 \text{ nm}$ thickness can be successfully isolated from the perennial scouring rush, *Equisetum hyemale*. We have shown that pure mesoporous amorphous silica with open surface area up to $400 \text{ m}^2/\text{g}$ can be obtained after leaching the plant with HCl followed by a calcination treatment. The optimum calcination temperature appears to be around 500°C . Calcination of untreated *E. hyemale* causes a collapse of the biogenic silica structure which is mainly attributed to the detrimental action of alkali ions present in the native plant. An initial HCl treatment does not only efficiently remove all these inorganic impurities but additionally opens up the pore structure by partial and gentle elimination of amorphous biopolymers such as hemicelluloses and pectin, allowing a perfect structure preservation of the biogenic silica after calcination. The HCl treatment, which may still be optimized, is therefore the key step in producing low-cost, high-quality silica from *Equisetum hyemale*.

Acknowledgment. We thank I. Zenke and R. Rothe from the MPI for support with SAXS/XRD and N_2 sorption measurements, respectively. We are grateful to G. Bach and T. Glaubauf from the IFN Zeitz for XRF analysis of the specimens. Financial support from the Max Planck society is gratefully acknowledged.

CM702991F

(28) Bassett, D. R.; Boucher, E. A.; Zettlemo, A. *J. Mater. Sci.* **1972**, *7* (12), 1379–1382.

(29) Real, C.; Alcala, M. D.; Munoz-Paez, A.; Criado, J. M. *Nucl. Instrum. Methods. Phys. Res., Sect. B* **1997**, *133* (1–4), 68–72.

(30) Krishnarao, R. V.; Subrahmanyam, J.; Kumar, T. J. *J. Eur. Ceram. Soc.* **2001**, *21* (1), 99–104.